was involved in suppression of virus production during the HR. On the other hand, induction of pathenogenesis-related (PR) proteins, PR-1 and PR-2, continued after the temperature shift in the *VPE*-silenced leaves as in the non-silenced plants (Fig. 4B). The *VPE* deficiency did not affect the production of the PR proteins, although it affected TMV-induced cell death. These results suggest that PCD and defense-protein induction are not coupled during the HR and that the HR is composed of two independent processes, PCD and defense-protein induction. VPE regulates PCD but not defense-protein induction. There has been a lot of discussion about whether PCD during the HR is really critical for resistance (*25*). Our results suggest that PCD contributes to resistance to a virus infection.

Although the *Arabidopsis* genome does not have a caspase family, it has a metacaspase family, which is distantly related to the caspase family. A metacaspase was reported to be involved in the cell death of yeast (*26*). The gene expression of metacaspase was found in pathogen-infected tomato leaves (*27*), and a proteolytic activity toward Ac-VEID-MCA (a metacaspase/caspase-6 substrate) was detected in dying suspensor cells of Norway spruce (*28*). Metacaspases might function in the cytosol during cell death as animal caspases. This is in contrast to the VPE functions in vacuole-mediated cell death. VPE is structurally unrelated to the caspase family, although it has caspase-1 activity and an ability to bind caspase-1 inhibitor.

In animals, dying cells are engulfed by phagocytes. However, in plants, which do not have phagocytes, cells surrounded by rigid cell walls must degrade their materials by themselves. Vacuolar collapse has been shown to trigger degradation of the cytoplasmic structures and lead to cell death (*21*), although its molecular mechanism is not known. Our findings suggest that VPE functions as a key player in vacuolar collapse–triggered cell death. VPEs are distributed in mono- and dicotyledonous plants. *Arabidopsis VPE* genes are up-regulated in dying cells during development and senescence of tissues (*5*, *13*). Thus, VPE might regulate various types of PCD in higher plants. Identification of the VPE-target proteins, which are possibly associated with the vacuolar membranes, would help to unravel the molecular mechanism of VPE-mediated vacuolar collapse underlying plant PCD. Because VPE acts as a processing enzyme to activate various vacuolar proteins, it might also convert the inactive hydrolytic enzymes to the active forms, which are involved in the disintegration of vacuoles, to initiate the proteolytic cascade in plant PCD. Understanding the VPE-regulated mechanism, which operates in the early process of the HR, may also lead to practical applications for strengthening disease resistance in crops.

References and Notes

1. G. M. Cohen, *Biochem. J.* **326**, 1 (1997).
2. E. Lam, O. del Pozo, *Plant Mol. Biol.* **44**, 417 (2000).
3. E. Lam, N. Kato, M. Lawton, *Nature* **411**, 848 (2001).
4. E. J. Woltering, A. van der Bent, F. A. Hoeberichts, *Plant Physiol.* **130**, 1764 (2002).
5. I. Hara-Nishimura, M. Maeshima, in *Vacuolar Compartments in Plants*, A. D. G. Robinson, J. C. Rogers, Eds. (Sheffield, London, 2000), pp. 20–42.
6. J. T. Greenberg, *Annu. Rev. Plant Physiol. Plant Mol. Biol.* **48**, 525 (1997).
7. I. Hara-Nishimura, K. Inoue, M. Nishimura, *FEBS Lett.* **294**, 89 (1991).
8. I. Hara-Nishimura, Y. Takeuchi, M. Nishimura, *Plant Cell* **5**, 1651 (1993).
9. K. Yamada, T. Shimada, M. Kondo, M. Nishimura, I. Hara-Nishimura, *J. Biol. Chem.* **274**, 2563 (1999).
10. N. Mitsuhashi *et al.*, *Plant Cell* **13**, 2361 (2001).
11. T. Shimada *et al.*, *J. Biol. Chem.* **278**, 32292 (2003).
12. K. Shirahama-Noda *et al.*, *J. Biol. Chem.* **278**, 33194 (2003).
13. T. Kinoshita, K. Yamada, N. Hiraiwa, M. Nishimura, I. Hara-Nishimura, *Plant J.* **19**, 43 (1999).
14. R. N. Goodman, A. J. Novacky, *The Hypersensitive Response Reaction in Plants to Pathogens: A Resistance Phenomenon* (American Phytopathological Society Press, St. Paul, MN, 1994).
15. N. Hiraiwa, M. Nishimura, I. Hara-Nishimura, *FEBS Lett.* **447**, 213 (1999).
16. M. Kuroyanagi, M. Nishimura, I. Hara-Nishimura, *Plant Cell Physiol.* **43**, 143 (2002).
17. S. M. Angell, D. C. Baulcombe, *Plant J.* **20**, 357 (1999).
18. I. Hara-Nishimura, in *Handbook of Proteolytic Enzymes*, A. J. Barrett, N. D. Rawlings, J. F. Woessner, Eds. (Academic Press, London, 1998), pp. 746–749.
19. I. Hara-Nishimura, T. Kinoshita, N. Hiraiwa, M. Nishimura, *J. Plant Physiol.* **152**, 668 (1998).
20. C. Becker *et al.*, *Eur. J. Biochem.* **228**, 456 (1995).
21. A. M. Jones, *Plant Physiol.* **125**, 94 (2001).
22. N. Hatsugai *et al.*, unpublished data.
23. R. Mittler, L. Simon, E. Lam, *J. Cell Sci.* **110**, 1333 (1997).
24. A. Levine, R. I. Pennell, M. E. Alvarez, R. Palmer, C. Lamb, *Curr. Biol.* **6**, 427 (1996).
25. J. T. Greenberg, N. Yao, *Cell. Microbiol.* **6**, 201 (2004).
26. F. Madeo *et al.*, *Mol. Cell* **9**, 911 (2002).
27. F. A. Hoeberichts, A. ten Have, E. J. Woltering, *Planta* **217**, 517 (2003).
28. P. V. Bozhkov *et al.*, *Cell Death Differ.* **11**, 175 (2004).

29. We thank B. Baker (University of California and USDA–Agriculture Research Service) for donating a binary vector with the TMV resistance gene *N*, D. C. Baulcombe (John Innes Centre, UK) for donating a *Potato virus X* vector (pgR107), and T. Kobayashi (National Institute for Basic Biology, Japan) for his help on pulsed-field gel electrophoresis. Supported by Core Research for Evolutional Science and Technology (CREST) of the Japan Science and Technology Corporation, and by Grants-in-Aid for Scientific Research (no. 12138205) and for 21st Century Center of Excellence Research, Kyoto University (A14), from the Ministry of Education, Culture, Sports, Science and Technology of Japan.

Supporting Online Material

www.sciencemag.org/cgi/content/full/305/5685/855/DC1
Materials and Methods
SOM Text
Figs. S1 and S2
References and Notes

3 May 2004; accepted 9 July 2004

Structural Basis of Mitochondrial Tethering by Mitofusin Complexes

Takumi Koshiba,[1] Scott A. Detmer,[1] Jens T. Kaiser,[2,3] Hsiuchen Chen,[1] J. Michael McCaffery,[4] David C. Chan[1*]

Vesicle fusion involves vesicle tethering, docking, and membrane merger. We show that mitofusin, an integral mitochondrial membrane protein, is required on adjacent mitochondria to mediate fusion, which indicates that mitofusin complexes act in trans (that is, between adjacent mitochondria). A heptad repeat region (HR2) mediates mitofusin oligomerization by assembling a dimeric, antiparallel coiled coil. The transmembrane segments are located at opposite ends of the 95 angstrom coiled coil and provide a mechanism for organelle tethering. Consistent with this proposal, truncated mitofusin, in an HR2-dependent manner, causes mitochondria to become apposed with a uniform gap. Our results suggest that HR2 functions as a mitochondrial tether before fusion.

Diverse membrane trafficking systems—including endoplasmic reticulum–to–Golgi transport, endosome fusion, Golgi-to-Golgi fusion, and synaptic vesicle fusion—use a common set of steps to mediate the targeting and fusion of intracellular vesicles to acceptor target membranes (*1*, *2*). First, a vesicle becomes "tethered" to its target membrane, although the two membranes remain separated by a considerable gap. This step is often mediated by the binding of activated Rab guanosine triphosphatases (GTPases) on the vesicle surface to effectors on the target membrane (*3*). Second, a SNARE (soluble *N*-ethylmaleimide–sensitive factor attachment protein receptor) protein on the tethered vesicle surface forms a complex with SNAREs on the target membrane; this leads to closer apposition of membranes, a state termed "docking." Finally, the two bilayers fuse, probably because of the close proximity produced by SNARE complex

[1]Division of Biology, [2]Division of Chemistry, California Institute of Technology, 1200 East California Boulevard, MC114-96, Pasadena, CA 91125, USA. [3]Howard Hughes Medical Institute. [4]Integrated Imaging Center, Department of Biology, Johns Hopkins University, 3400 North Charles Street, Baltimore, MD 21218, USA.

*To whom correspondence should be addressed. E-mail: dchan@caltech.edu

formation. Although much progress has been made in understanding the structural basis of docking and fusion by SNARE complexes (*4*, *5*), less is understood about tethering, because of difficulty in obtaining structures of the large heterotypic protein complexes involved.

Mitochondria are dynamic organelles that undergo continual cycles of fusion and fission, opposing processes that control the overall morphology of the mitochondrial population (*6*–*8*). Reduced mitochondrial fusion causes greater autonomy for individual organelles in the mitochondrial population, a state that increases heterogeneity among organelles and results in dysfunction (*9*). Mitochondrial fusion is controlled by members of the *fuzzy onions* (Fzo)/mitofusin (Mfn) family of large GTPases that are localized to the mitochondrial outer membrane (*10*). Mammals have two mitofusins, Mfn1 and Mfn2 (*9*, *11*–*14*), that control mitochondrial fusion and are required for embryonic development (*9*). Mutations in *Mfn2* are responsible for most cases of Charcot-

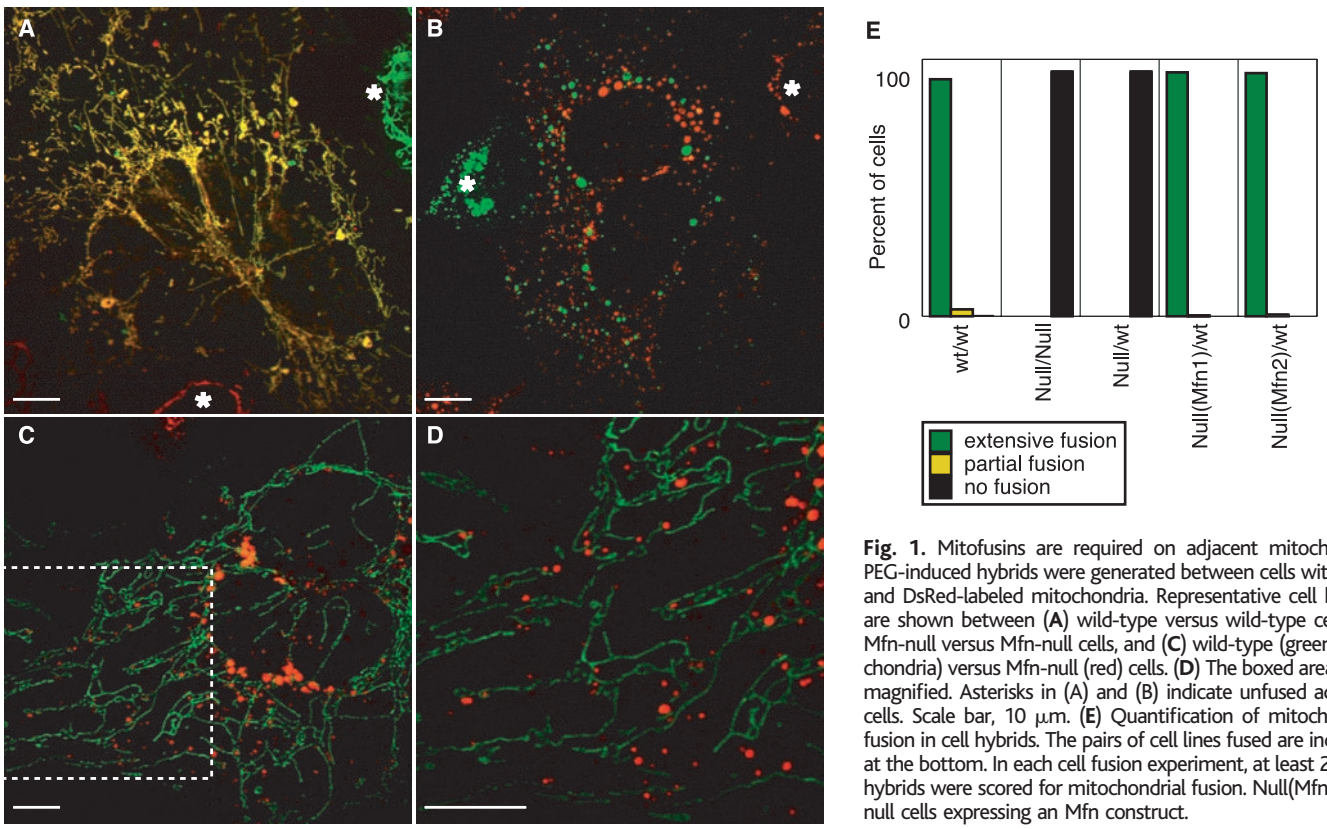

Fig. 1. Mitofusins are required on adjacent mitochondria. PEG-induced hybrids were generated between cells with GFP- and DsRed-labeled mitochondria. Representative cell hybrids are shown between (**A**) wild-type versus wild-type cells, (**B**) Mfn-null versus Mfn-null cells, and (**C**) wild-type (green mitochondria) versus Mfn-null (red) cells. (**D**) The boxed area in (C) magnified. Asterisks in (A) and (B) indicate unfused adjacent cells. Scale bar, 10 μm. (**E**) Quantification of mitochondrial fusion in cell hybrids. The pairs of cell lines fused are indicated at the bottom. In each cell fusion experiment, at least 250 cell hybrids were scored for mitochondrial fusion. Null(Mfn), Mfn-null cells expressing an Mfn construct.

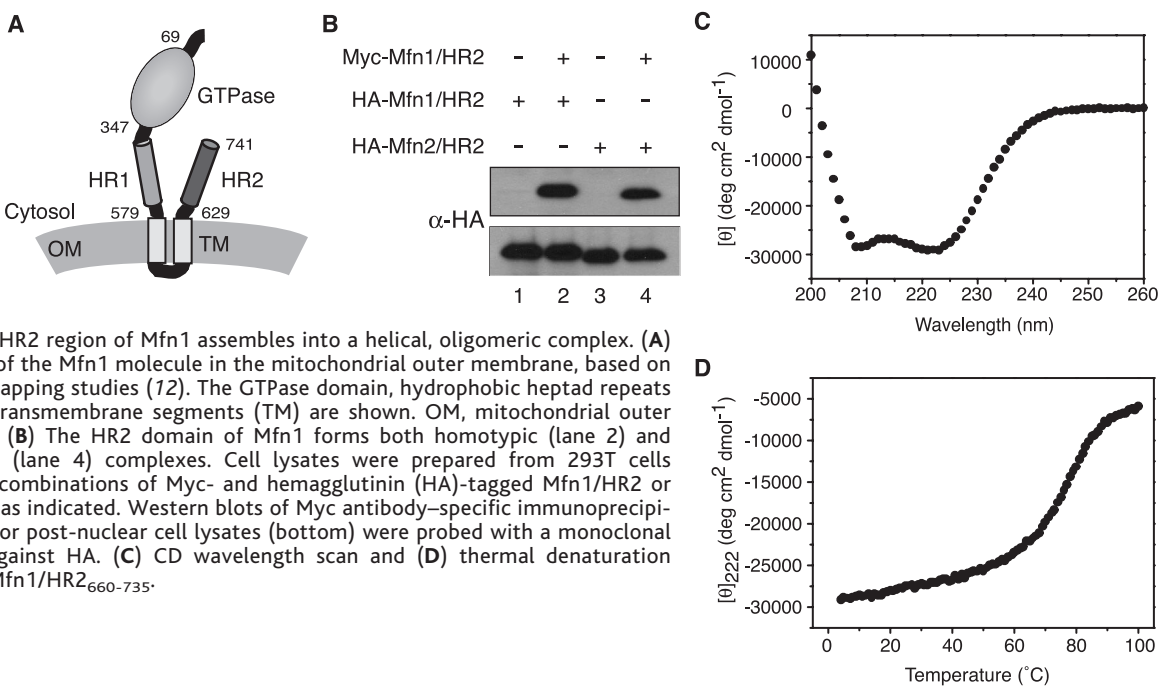

Fig. 2. The HR2 region of Mfn1 assembles into a helical, oligomeric complex. (**A**) Schematic of the Mfn1 molecule in the mitochondrial outer membrane, based on topology mapping studies (*12*). The GTPase domain, hydrophobic heptad repeats (HR), and transmembrane segments (TM) are shown. OM, mitochondrial outer membrane. (**B**) The HR2 domain of Mfn1 forms both homotypic (lane 2) and heterotypic (lane 4) complexes. Cell lysates were prepared from 293T cells expressing combinations of Myc- and hemagglutinin (HA)-tagged Mfn1/HR2 or Mfn2/HR2, as indicated. Western blots of Myc antibody–specific immunoprecipitates (top) or post-nuclear cell lysates (bottom) were probed with a monoclonal antibody against HA. (**C**) CD wavelength scan and (**D**) thermal denaturation profile of $Mfn1/HR2_{660\text{-}735}$.

Marie-Tooth type 2A disease, an inherited peripheral neuropathy (*15*). In spite of these insights, it is not known whether mitofusins directly mediate fusion and whether this process proceeds through the canonical steps of tethering, docking, and fusion.

To address this issue, we examined whether mitofusins are required on adjacent mitochondria during homotypic membrane fusion. Mitochondrial fusion in mammalian cells can be measured in vivo by using polyethylene glycol (PEG) to generate cell hybrids between cell lines with differentially marked mitochondria (*16*). When wild-type mouse embryonic fibroblasts with either mitochondrially targeted green fluorescent protein (GFP) or DsRed are fused in this manner, the vast majority of cell hybrids (97%) show extensively fused mitochondria by 7 hours (Fig. 1, A and E). We next tested fibroblasts containing targeted deletions in both *Mfn1* and *Mfn2*. Such Mfn-null cells have completely fragmented mitochondria and show no detectable mitochondrial fusion (Fig. 1, B and E). In contrast, cells null for only Mfn1 or Mfn2 contain low but readily measured rates of fusion, with many hybrids showing partially fused mitochondrial populations (*9*). These results indicate that mitofusins are absolutely required for mitochondrial fusion. Most important, cell hybrids between Mfn-null cells and wild-type cells show no detectable mitochondrial fusion (Fig. 1, C to E). In such hybrids, the mitochondria derived from wild-type cells remain elongated tubules, clearly distinct from the spherical mitochondria derived from mutant cells. Reintroduction of either *Mfn1* or *Mfn2* into Mfn-null cells fully rescues mitochondrial fusion in cell hybrids with wild-type cells (Fig. 1E). These observations indicate that mitochondrial fusion requires mitofusins on adjacent mitochondria. Because these outer membrane proteins form both homotypic and heterotypic complexes (*9*), the most likely explanation is that fusion requires mitofusin complexes acting in trans (that is, between adjacent mitochondria) (*17*–*19*).

We therefore attempted to identify domains of mitofusin that might mediate oligomerization. Both Mfn1 and Mfn2 contain two 4,3 hydrophobic heptad repeats (HR1 and HR2) that flank the bipartite transmembrane segment (Fig. 2A). Heptad repeats play central roles in membrane fusion mediated by SNARE proteins and many viral envelope glycoproteins (*1*, *20*). Using immunoprecipitation, we found that isolated HR2 fragments expressed in 293T cells form stable complexes (Fig. 2B). Mfn1/HR2 forms stable complexes with itself, as well as with Mfn2/HR2. Therefore, the HR2 region can form homotypic and heterotypic complexes, which parallel the behavior of full-length Mfn1 and Mfn2 (*9*).

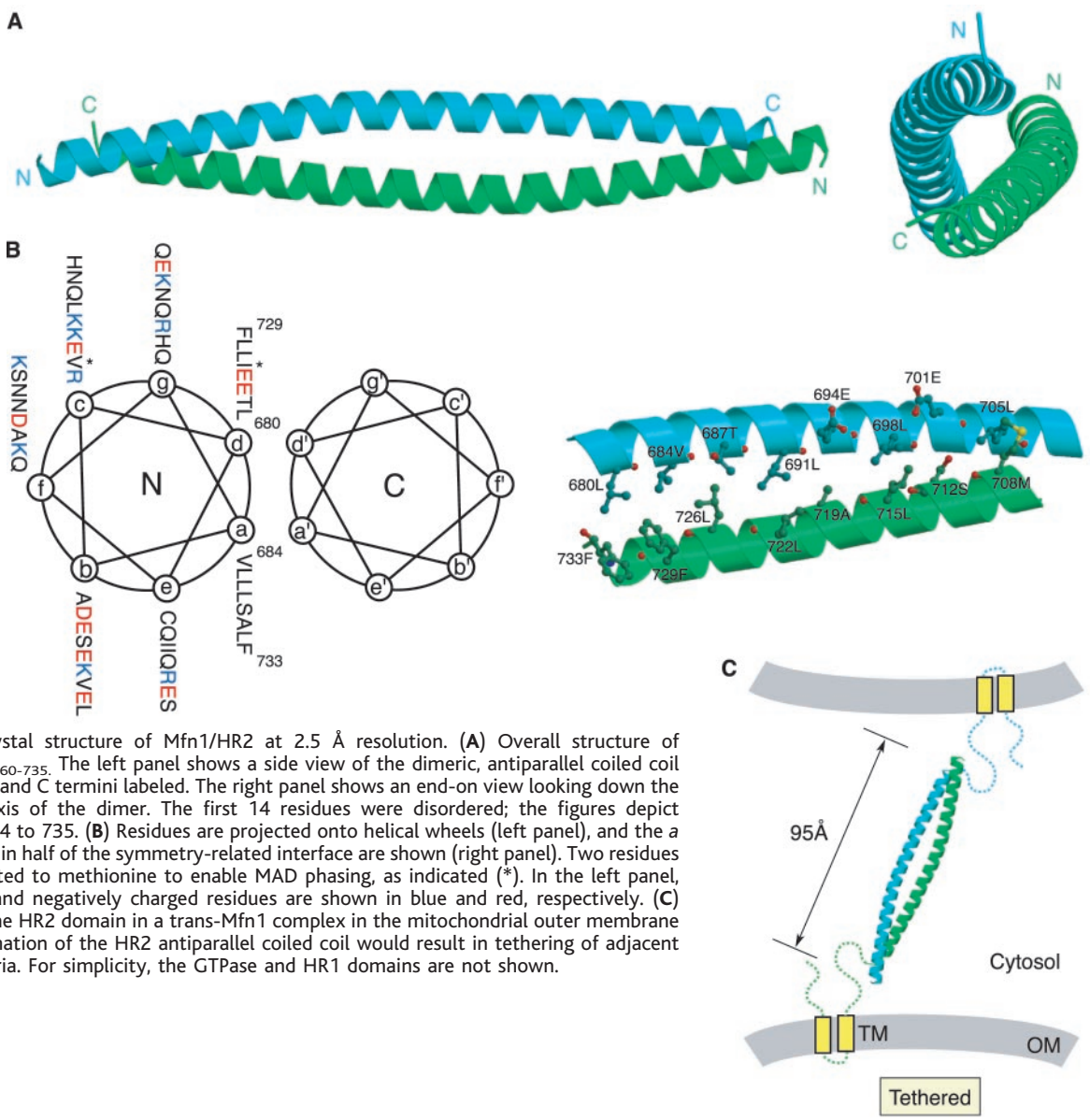

Fig. 3. Crystal structure of Mfn1/HR2 at 2.5 Å resolution. (**A**) Overall structure of Mfn1/HR2$_{660-735}$. The left panel shows a side view of the dimeric, antiparallel coiled coil with the N and C termini labeled. The right panel shows an end-on view looking down the two-fold axis of the dimer. The first 14 residues were disordered; the figures depict residues 674 to 735. (**B**) Residues are projected onto helical wheels (left panel), and the *a* to *d'* layers in half of the symmetry-related interface are shown (right panel). Two residues were mutated to methionine to enable MAD phasing, as indicated (*). In the left panel, positively and negatively charged residues are shown in blue and red, respectively. (**C**) Model of the HR2 domain in a trans-Mfn1 complex in the mitochondrial outer membrane (OM). Formation of the HR2 antiparallel coiled coil would result in tethering of adjacent mitochondria. For simplicity, the GTPase and HR1 domains are not shown.

We investigated the biophysical properties of the Mfn1/HR2 region. Recombinant Mfn1/HR2 was subjected to limited proteolysis with a panel of proteases to yield a slightly smaller, stable domain (residues 660 to 735) that corresponded well with the predicted heptad repeat (fig. S1, A and B). The resulting fragment, Mfn1/HR2$_{660\text{-}735}$, retains self-association in an immunoprecipitation assay (fig. S1C). Mfn1/HR2$_{660\text{-}735}$ appears to be well folded, because circular dichroism (CD) analysis indicates that it is highly helical (77%) and unfolds cooperatively, with a thermal transition midpoint of 78°C (Fig. 2, C and D).

We obtained crystals of Mfn1/HR2$_{660\text{-}735}$ and solved its atomic structure at 2.5 Å by multiwavelength anomalous diffraction (MAD) analysis of a selenomethionine-substituted crystal (table S1 and fig. S2). The HR2 polypeptide folds into a dimeric antiparallel coiled coil that is 95 Å long (Fig. 3A). Each of the two helices can be depicted in a helical wheel diagram (Fig. 3B), from which it can be readily observed that the *a* and *d* residues of the heptad repeat constitute a predominantly hydrophobic interaction interface. Complex formation involves typical "knobs-in-holes" packing, buries 2850 Å^2 of surface area, and results in a highly charged surface (fig. S3A).

An interesting feature of this coiled coil is the presence of two glutamic acids at consecutive *d* positions (Glu^{694} and Glu^{701}). These two charged residues may be important in specifying the antiparallel orientation of the HR2 coiled coil. In fact, the addition of a charged residue in the *d* position has been used as part of a design strategy to construct artificial coiled coils with a strong tendency for the antiparallel orientation (*21*, *22*). Among mitofusin homologs, these *d* positions contain either charged or polar residues (fig. S3B). Substitution of these positions with leucines reduces the ability of Mfn1 to restore tubular mitochondrial morphology in Mfn-null cells (fig. S4).

To test whether the HR2 coiled coil is essential for mitofusin function, we designed mutations expected to disrupt its structure. We introduced proline substitutions into recombinant Mfn1/HR2$_{660\text{-}735}$ at positions 691 and 705. CD, gel filtration, and immunoprecipitation analysis indicate that both mutations significantly reduce the stability of the HR2 coiled coil, with the proline replacement of leucine at residue 705 (L705P) much more severe than L691P (fig. S5). We studied the effects of these mutations on the ability of Mfn1 to restore mitochondrial tubules to Mfn-null cells. Expression of wild-type Mfn1 fully rescues the fragmented mitochondria of Mfn-null cells (Fig. 4A). Mfn1(L691P) can restore a subset of the mitochondrial population to tubules, but almost no cells show the fully tubular mitochondrial morphology observed with wild-type Mfn1. This result is consistent with the moderate effect of this mutation on the biophysical properties of Mfn1/HR2$_{660\text{-}735}$ (fig. S5). In contrast, the L705P mutant has little activity in vivo (Fig. 4A). Corresponding defects in mitochondrial fusion activity were observed using the PEG cell hybrid assay (Fig. 4B). Both mutants retain predominantly mitochondrial localization (fig. S6). These results indicate that the HR2 coiled coil is essential for the mitochondrial fusion activity of Mfn1.

Because of the antiparallel orientation of the HR2 coiled coil, a remarkable consequence is that the membrane-anchoring segments of mitofusin dimers would be located at opposite ends of the 95 Å coiled coil (Fig. 3C). In addition, there are more than 40 residues between each transmembrane anchor and the beginning of the coiled coil. In a trans complex of mitofusin dimers, this coiled coil would lock two mitochondria together but would likely leave a significant gap between the opposing outer membranes. It is not possible to predict precisely the dimensions of such a gap, because it would depend on the angle of the coiled coil in relation to the opposing bilayers.

In the course of examining the role of the GTPase domain of Mfn1, we found that amino terminal truncations that remove the GTPase domain result in extensive aggregation of mitochondria when expressed in NIH 3T3 cells (Fig. 4, C and D). Some constructs of human Mfn1 also cause mitochondrial aggregation (*14*), although it is unclear whether that effect is related to the results described here. The aggregation by truncated Mfn1 (residues 331 to 741)

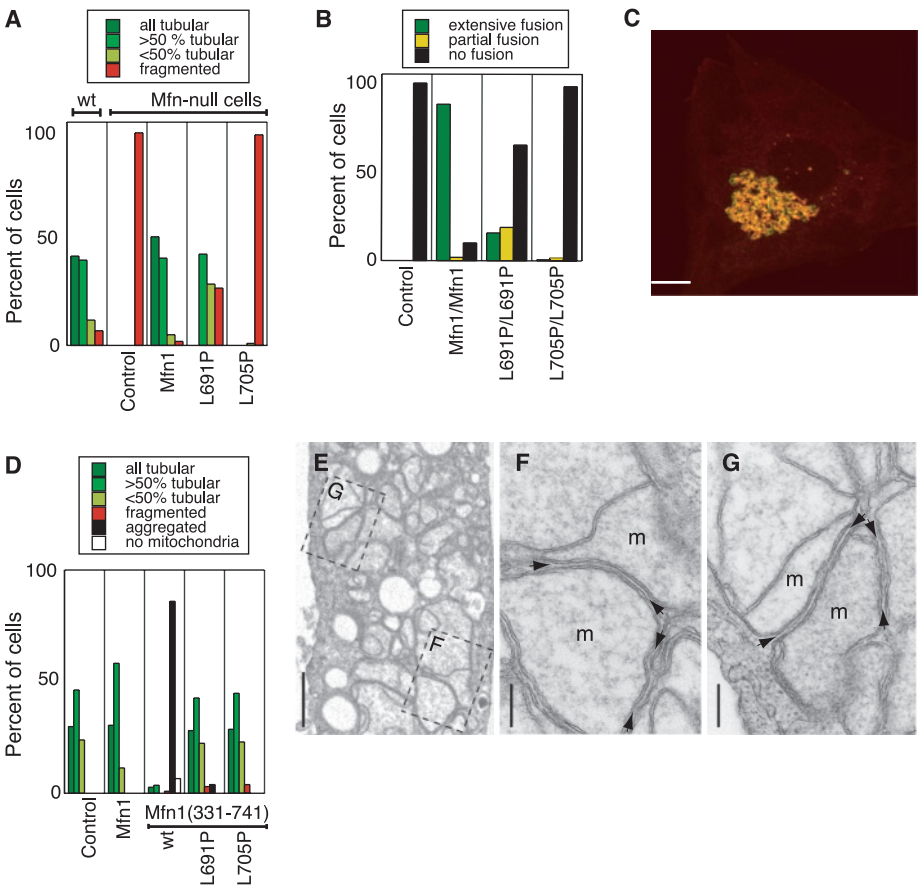

Fig. 4. Disruption of HR2 structure abolishes mitochondrial fusion by Mfn1 and mitochondrial tethering by truncated Mfn1. (**A**) Mitochondrial morphologies in Mfn-null mouse embryo fibroblasts (MEFs) infected with retrovirus expressing Myc-tagged Mfn1 mutants. (Left) For comparison, data from a wild-type cell line are also presented. Mitochondrial morphology is scored by mitochondrially targeted GFP, and infected cells were identified by immunofluorescence against the Myc tag. Control, empty retrovirus. (**B**) PEG fusion assay of Mfn1 mutants. Wild-type or mutant Mfn1 was expressed in Mfn-null cells. PEG-induced hybrids were generated between cells containing the same construct. Control, empty retrovirus. (**C**) Mitochondrial aggregation in an NIH 3T3 cell expressing truncated Mfn1 (Myc-tagged). Mitochondria are visualized by mitochondrially targeted GFP, and truncated Mfn1 by immunofluorescence (Cy3) against the Myc epitope. Scale bar, 10 μm. (**D**) Mitochondrial morphologies in NIH 3T3 cells infected with retrovirus expressing truncated Mfn1 (residues 331 to 741) or derivatives with HR2 mutations. Control, empty retrovirus. (**E**) Electron micrograph of mitochondrial tethering by truncated Mfn1. Scale bar, 1 μm. Rectangles indicate regions magnified in (**F**) and (**G**). Note the uniform gap (arrowheads) between adjacent double-membraned mitochondria (m). Scale bar, 0.2 μm.

is dependent on HR2 coiled-coil formation, because HR2-destabilizing mutations abolish the effect (Fig. 4D). Strikingly, electron microscopy revealed densely packed mitochondria that maintain a uniform gap between opposing outer mitochondrial membranes (Fig. 4, E to G). The average distance of this gap is 159 Å (n = 124 measurements; SD = 30 Å). Taken together, these results suggest that, in the absence of the GTPase domain, Mfn1 is unable to promote full fusion. Instead, mitochondria are trapped in a tethered state mediated by the HR2 coiled coil. At present, we do not know if this trapped state remains competent for future fusion.

Because mitofusins are required on the outer membranes of adjacent mitochondria, it is likely that they act in trans and are directly involved in promoting membrane fusion. Moreover, our results suggest that mitochondrial fusion, like other intracellular membrane fusion events, proceeds through a tethering step before full fusion. The HR2 structure provides a structural understanding of how antiparallel coiled-coil formation can mediate organelle tethering by providing a large interaction interface while maintaining separation of the membrane anchors. In contrast, trans-SNARE complexes drive membrane-anchoring regions into close apposition (*4*) and may force bilayer merger. Many of the components mediating vesicle tethering are known in other membrane-trafficking systems, but those tethering events are far more complex, involving heterotypic interactions between Rab GTPases and large, coiled coil–containing proteins (*3*). As a result, they are poorly understood structurally, even though crystal structures of some individual components are available (*23*).

The HR2 structure provides a mechanism for the tethering of mitochondria, rather than for the closer apposition that must occur later during the fusion process (Fig. 3C). It is likely that mitofusins themselves mediate these downstream events, because genomic screens for mitochondrial fusion molecules have failed to identify molecules, besides the Fzo/Mfn proteins, that are both located in the outer membrane and conserved in vertebrates (*24*). In future work, it will be critical to understand how further mitofusin-mediated structural rearrangements, likely involving regulation by the GTPase domain, lead to full fusion.

References and Notes

1. J. S. Bonifacino, B. S. Glick, *Cell* **116**, 153 (2004).
2. I. Mellman, G. Warren, *Cell* **100**, 99 (2000).
3. J. R. Whyte, S. Munro, *J. Cell Sci.* **115**, 2627 (2002).
4. R. B. Sutton, D. Fasshauer, R. Jahn, A. T. Brunger, *Nature* **395**, 347 (1998).
5. T. Weber *et al.*, *Cell* **92**, 759 (1998).
6. H. Chen, D. C. Chan, *Curr. Top. Dev. Biol.* **59**, 119 (2004).
7. M. Karbowski, R. J. Youle, *Cell Death Differ.* **10**, 870 (2003).
8. J. M. Shaw, J. Nunnari, *Trends Cell Biol.* **12**, 178 (2002).
9. H. Chen *et al.*, *J. Cell Biol.* **160**, 189 (2003).
10. A. D. Mozdy, J. M. Shaw, *Nature Rev. Mol. Cell Biol.* **4**, 468 (2003).
11. A. Santel, M. T. Fuller, *J. Cell Sci.* **114**, 867 (2001).
12. M. Rojo, F. Legros, D. Chateau, A. Lombes, *J. Cell Sci.* **115**, 1663 (2002).
13. F. Legros, A. Lombes, P. Frachon, M. Rojo, *Mol. Biol. Cell* **13**, 4343 (2002).
14. A. Santel *et al.*, *J. Cell Sci.* **116**, 2763 (2003).
15. S. Zuchner *et al.*, *Nature Genet.* **36**, 449 (2004).
16. Materials and methods are available as supporting materials on *Science* Online.
17. A previous study using RNA interference to reduce mitofusin levels in rat cells concluded that mitofusins function in cis (on a single mitochondrial membrane) (*18*). These authors found that fusion of wild-type and mitofusin knockdown cells resulted in significant fusion of mitochondria. However, it is clear that the RNA interference in that study failed to completely deplete both mitofusins, because residual mitochondrial fusion was observed even in cell hybrids between double mitofusin knockdown cells [figure 5 of (*18*)]. In our study, the use of genetically defined, Mfn-null cells leads to definitive results. Yeast mitochondrial fusion also requires Fzo1 on adjacent membranes, on the basis of an in vitro mitochondrial fusion assay (*19*).
18. N. Ishihara, A. Jofuku, Y. Eura, K. Mihara, *Biochem. Biophys. Res. Commun.* **301**, 891 (2003).
19. S. Meeusen, J. M. McCaffery, J. Nunnari, manuscript in preparation.
20. D. M. Eckert, P. S. Kim, *Annu. Rev. Biochem.* **70**, 777 (2001).
21. M. G. Oakley, J. J. Hollenbeck, *Curr. Opin. Struct. Biol.* **11**, 450 (2001).
22. D. G. Gurnon, J. A. Whitaker, M. G. Oakley, *J. Am. Chem. Soc.* **125**, 7518 (2003).
23. J. J. Dumas *et al.*, *Mol. Cell* **8**, 947 (2001).
24. K. S. Dimmer *et al.*, *Mol. Biol. Cell* **13**, 847 (2002).

25. We are grateful to D. Rees, J. Nunnari, and R. Deshaies for helpful discussions. We thank the staff of the Advanced Light Source at Berkeley Lab. We thank P. Huang for advice on structural analysis. T.K. was supported by a Gosney Foundation postdoctoral fellowship; J.T.K. is an HHMI Research Associate. This work was supported by the National Institute of Health (R01 GM62967). D.C.C. is a Bren Scholar, Rita Allen Scholar, and Beckman Young Investigator. Atomic coordinates and structure factors have been deposited in the Protein Data Bank, accession code 1T3J.

Supporting Online Material

www.sciencemag.org/cgi/content/full/305/5685/858/DC1
Materials and Methods
Figs. S1 to S6
Table S1
References

30 April 2004; accepted 30 June 2004 .

The Semaphorin 4D Receptor Plexin-B1 Is a GTPase Activating Protein for R-Ras

Izumi Oinuma, Yukio Ishikawa, Hironori Katoh, Manabu Negishi*

Plexins are cell surface receptors for semaphorin molecules, and their interaction governs cell adhesion and migration in a variety of tissues. We report that the Semaphorin 4D (Sema4D) receptor Plexin-B1 directly stimulates the intrinsic guanosine triphosphatase (GTPase) activity of R-Ras, a member of the Ras superfamily of small GTP-binding proteins that has been implicated in promoting cell adhesion and neurite outgrowth. This activity required the interaction of Plexin-B1 with Rnd1, a small GTP-binding protein of the Rho family. Down-regulation of R-Ras activity by the Plexin-B1-Rnd1 complex was essential for the Sema4D-induced growth cone collapse in hippocampal neurons. Thus, Plexin-B1 mediates Sema4D-induced repulsive axon guidance signaling by acting as a GTPase activating protein for R-Ras.

Plexins constitute a large family of transmembrane proteins that function as receptors for semaphorins (*1*). Semaphorins were originally identified as repulsive axonal guidance molecules in the developing nervous system, but have recently been shown to control cell adhesion and migration in other tissues (*2*–*5*). The cytoplasmic domain of plexin family members has been highly conserved during evolution and shares sequence similarity with Ras family–specific GTPase activating proteins (GAPs), especially R-Ras GAP (*6*, *7*). These homologous domains in plexins contain two conserved arginine residues corresponding to those essential for the catalytic activity of common Ras GAPs (*8*); however, no GAP activity by plexins has been demonstrated so far. R-Ras has been shown to play a key role in cell adhesion by activating integrins and to promote cell migration and neurite outgrowth (*9*–*12*).

Rnd1, a constitutively active Rho family member (*13*), directly interacts with Plexin-B1, the receptor for Semaphorin 4D (Sema4D) (*14*). The Rnd1-binding region in Plexin-B1 is located between the two GAP-homologous domains (Fig. 1E). To evaluate whether the interaction of Rnd1 with Plexin-B1 could affect the GAP activity toward R-Ras, we examined the interaction between Plexin-B1 and R-Ras in the presence and the absence of Rnd1. Epitope (Myc)–tagged cy-

Laboratory of Molecular Neurobiology, Graduate School of Biostudies, Kyoto University, Sakyo-ku, Kyoto 606-8502, Japan.

*To whom correspondence should be addressed. E-mail address: mnegishi@pharm.kyoto-u.ac.jp